

# Surface Quality of AZ91D Magnesium Alloy After Precision Milling with Coated Tools

Jarosław Korpysa\* – Józef Kuczmaszewski – Ireneusz Zagórski  
Lublin University of Technology, Faculty of Mechanical Engineering, Poland

*This study investigates the surface quality of AZ91D magnesium alloy specimens after precision milling. The milling was conducted with the use of TiB<sub>2</sub>- and TiAlN-coated carbide end mills. The following variables were used in the milling process: cutting speed  $v_c$ , feed per tooth  $f_z$  and axial depth of cut  $a_p$ . The surface quality was analysed based on surface roughness parameters and Abbott-Firestone curves. The results showed that the surface quality after machining depended on the tool coating type and applied machining parameters; the only exception was the axial depth of cut because changes in its value did not have any significant effect on the obtained surface quality. After precision milling, AZ91D specimens were characterized by very low surface roughness parameters. The impact of machining conditions was also evaluated with ANOVA analysis, which confirmed the significant effect of cutting speed and feed per tooth. It also indicated the dependence of the roughness parameters on the tool coating type. The tool coating type and machining conditions did not have any significant effect on the Abbott-Firestone curves. Despite the changes applied, the shape of the curves remained similar. The obtained results provide both theoretical and practical knowledge about the achievable surface roughness of AZ91D magnesium alloy specimens after precision milling.*

**Keywords:** precision milling, surface quality, Abbott-Firestone curve, ANOVA, coated tools

## Highlights

- Precision milling of AZ91D magnesium alloy enables the formation of high-quality surfaces with low roughness parameter values.
- The effect of a change in process parameters on surface roughness depends on the tool coating type.
- The changes in the cutting speed and feed per tooth have a significant influence on the surface roughness parameters, validated by ANOVA analysis.
- Abbott-Firestone curves have a degressive-progressive shape, favourable in functional terms.

## 0 INTRODUCTION

Surface roughness is the main factor determining the quality of a machined surface. This is particularly important in precision machining, which is oriented at manufacturing high-accuracy parts; thus, any surface unevenness is an important factor of allowable dimensional and geometrical deviations. The achievement of a surface with the required quality is a very complex problem because it depends on many factors, such as machining strategy and conditions, cutting tool type or cooling conditions. Therefore, conducting research on the effects of individual factors on surface roughness to determine optimum machining conditions is of vital importance regardless of the machined material [1] to [5].

Among the most commonly applied surface roughness parameters is the arithmetic mean height  $R_a$ , belonging to the group of amplitude parameters. These parameters serve as a basis for evaluating surface texture and describing the roughness of machined surfaces quite well. It should, however, be stressed that the  $R_a$  parameter has no specific information about the shape of a surface roughness profile. Single peaks have an insignificant effect on this parameter. In effect, this parameter is an

absolute measure, which means that it does not take into account whether a given profile has valleys or peaks. Despite its shortcomings, this parameter is very useful for evaluating the stability and control of a technological process [6] to [7]. Another commonly studied surface roughness parameter is the total height of the roughness profile  $R_t$ , which is determined between the largest profile peak height and the largest profile valley depth.  $R_t$  is another amplitude-related parameter.  $R_t$  and  $R_z$  parameters also provide much more information on fatigue strength [8]. In addition, the  $R_t$  parameter can affect the functional properties of a surface, including fatigue strength, reflexivity, friction and wear, lubrication, mechanical strength, as well as assembly tolerances [9]. Still, for a comprehensive analysis of surface quality, it is necessary to examine the widest possible range of parameters, because an analysis of a single parameter will only provide basic information about surface texture. Surface topography is examined based on two-dimensional (2D) and three-dimensional (3D) parameters, surface topography maps or isotropy [10] to [12].

As previously mentioned, studies investigating surface roughness after machining usually focus on the  $R_a$  parameter. For example, a study [13]

\*Corr. Author's Address: Lublin University of Technology, Faculty of Mechanical Engineering, Poland, j.korpysa@pollub.pl

investigated changes in the  $Ra$  parameter after the AM60 magnesium alloy milling process with the use of a carbide end mill with TiN coatings. The  $Ra$  parameter value for optimal machining parameters was estimated to be approximately  $0.3 \mu\text{m}$ . In a study [14] devoted to face milling of AZ61 alloy with the use of a milling cutter with carbide inserts, the obtained  $Ra$  parameter ranged from  $0.1 \mu\text{m}$  to  $0.4 \mu\text{m}$ . A study [15] investigated the machinability of AZ61 alloy. The machining process was conducted with the use of a face milling cutter with carbide inserts, and the obtained  $Sa$  parameter values ranged approx.  $0.14 \mu\text{m}$  to  $0.8 \mu\text{m}$  (direct feed) and  $0.2 \mu\text{m}$  to  $0.7 \mu\text{m}$  (reversed feed). In a study [16], the authors performed high-speed machining using a face milling cutter, which made it possible to archive very low surface roughness of AZ91D alloy, with the  $Ra$  parameter ranging from  $0.06 \mu\text{m}$  to  $0.13 \mu\text{m}$ . A study on milling AZ31B alloy specimens [17] reported that the surface has deteriorated with increasing the feed per tooth and amount of cutting edges. Similar findings were obtained in a study [18], where the surface roughness parameter  $Ra$  increased due to an increase in the cutting speed as well as the feed per tooth. A study conducted on milling AZ31B alloy [19] demonstrated that a cutting zone cooling method was also of significant importance. The results of a milling process conducted with an AlTiN-coated carbide end mill with four cutting edges showed that the use of cryogenic cooling led to approximately 20 % lower  $Ra$  when compared to oil cooling. In another study [20], the milling of ZE41 alloy was performed using a face milling cutter with carbide inserts. It was found that the  $Ra$  parameter value primarily depended on the feed per tooth and the cutting speed ( $Ra$  ranged from approx.  $1.4 \mu\text{m}$  to  $4.1 \mu\text{m}$ ) and that an increase in their values led to increased surface roughness. Research on this magnesium alloy was also described in [21], in which the effect of different cutting parameters on surface roughness was analysed, although using a high-speed steel (HSS) tool. It was shown that increasing the feed per tooth and the depth of cut resulted in a linear increase in the  $Ra$  parameter, which varied from  $0.306 \mu\text{m}$  to  $0.679 \mu\text{m}$ .

Interesting results were also obtained in a study on Mg-SiC/B<sub>4</sub>C-reinforced magnesium matrix composite [22]. The lowest values of the  $Ra$  parameter range from approx.  $0.4 \mu\text{m}$  to  $0.5 \mu\text{m}$  were archived when machining was performed with a TiN-coated tool. A study [23] examined the influence of variable milling parameters on surface roughness. The milling process of AZ91 alloy was conducted with variable cutting speed, feed per tooth and depth of cut, using a 50

mm diameter face mill with carbide inserts. Obtained values of  $Ra$  parameter ranged from  $0.067 \mu\text{m}$  to  $0.208 \mu\text{m}$ , and the results showed that surface roughness primarily depended on the feed per tooth, which was also confirmed by ANOVA analysis. That line of research was continued in a study [24], which focused on the determination of optimum milling conditions by TOPSIS analysis based on vibration signals. The results also confirmed that reduced surface roughness primarily resulted from decreased feed per tooth. A more comprehensive analysis of AZ91D alloy surface roughness was conducted in [25], in which profile and areal roughness parameters and surface topography maps were taken into consideration. The results showed that the surface quality of AZ91D alloy specimens milled using a TiAlN-coated carbide tool could considerably be improved by changing values of the cutting speed and feed per tooth.

Improved surface quality can also be obtained by using top-quality carbide milling end mills, as well as tools with cutting edges made of polycrystalline diamond (PCD). To give an example, for the face milling process of Mg-Ca0.8 alloy elements, the obtainable  $Ra$  values can range from  $0.2 \mu\text{m}$  to  $0.8 \mu\text{m}$  if PCD face mills are used [26].  $Ra$  parameter values of approx.  $0.4 \mu\text{m}$  were also obtained by combined dry milling and burnishing [27] and [28]. In a study [29], which was conducted on milling Mg-Ca0.8 alloy specimens using a face mill with uncoated carbide inserts, the obtained  $Ra$  values were from  $0.9 \mu\text{m}$  to  $1.4 \mu\text{m}$  during normal milling and from  $0.09 \mu\text{m}$  to  $0.8 \mu\text{m}$  during inverse milling. In a study [30] investigating the Mg-Ca1.0 alloy in a milling process conducted using a face mill with diamond-like carbon (DLC)-coated inserts, the obtained surface roughness parameter  $Ra$  values ranged from  $0.10 \mu\text{m}$  to  $0.16 \mu\text{m}$ . The cooling method used may also have a significant impact on the machining effect. Jouini et al. [31] proved in their paper that the use of cryogenic cooling for AZ91D magnesium alloy machining can result in a significant improvement in surface quality. However, the improvement only occurred under specific conditions. Minimum quantity lubrication (MQL) can also be an effective cooling method. Research presented in [32] indicated that surface roughness could also be reduced using this method, but it was less effective than changing the cutting speed.

In addition to using basic surface roughness parameters, which are well-known and widely used, surface quality can also be evaluated based on the Abbott-Firestone curve and parameters describing this curve. The use of these parameters is a different approach to surface texture evaluation, one that can

effectively be employed to evaluate the quality of surfaces obtained by different machining methods [33] to [35]. Material ratio curves were used, for instance, in the paper [36]. The curves obtained on the surfaces of the AZ91D alloy had mostly a degressive-progressive shape, while changes in machining conditions mainly caused a change in their inclination. The course of the curves also looked similar after trochoidal milling of AZ91D and AZ31 alloys [37]. The curves flattened when the cutting speed was increased, and the trochoidal step was reduced. Trochoidal milling was also performed in the paper [38], analysing Incoloy 800 surfaces. Increasing the feed rate resulted in an increase in the values of the  $Spk$  and  $Sk$  parameters, while the trochoidal stepover mainly increased the  $Spk$  parameter. Based on the curve shape, one can infer the tribological wear resistance of a given surface. A progressive shape of the curve means that the analysed surface has rounded peaks and is more wear-resistant than surfaces described by degressive shape curves. The curve shape is described by parameters, which are determined based on that curve. These parameters include reduced peak height  $Rpk$ , reduced valley depth  $Rvk$  and core roughness depth  $Rk$ . Based on these parameters, one can predict the influence of surface texture on the operational aspects of machine components [39] and [40]. The effect of reduced friction can also occur when the reduced valley depth  $Rvk$  is higher than the reduced peak height  $Rpk$  [8] and [41]. The material contribution curves in the case of AZ61 alloy were also used to analyse dry sliding wear behaviour [42].

According to the presented review of recent publications in the field of magnesium alloy milling, a considerable number of papers are limited to the analysis of only one surface roughness parameter. Such an approach is highly inadequate, and this does not allow an appropriate description of the surface quality. A more comprehensive representation of the surface is only possible after analysis of more parameters, including functional parameters. Furthermore, all these papers concern conventional machining, whereas the research described in the present paper involves precision milling, which is the main novelty of this study. The application of precision milling for magnesium alloy machining has hardly been used thus far, which is confirmed by the very small number of available publications on this subject. Due to the different machining process mechanics under these machining conditions, the results obtained in conventional machining cannot be directly transferred to precision machining, so that requires separate research. The main objective of the

research is, therefore, to obtain a knowledge base on the impact of cutting factors such as technological conditions or tool coating type on surface roughness. An important element of the paper is also the analysis of functional parameters and Abbott-Firestone curves to evaluate the surface in terms of possible component interaction. The effect of the various cutting parameters and tool coating type on surface roughness was also assessed using ANOVA.

## 1 EXPERIMENTAL

This study involved conducting the milling process under precision machining conditions and evaluating the obtained surface quality. Test specimens were made of the AZ91D magnesium alloy. This is one of the most widely applied magnesium alloys in many industrial branches. The machining process was performed on the AVIA VMC 800HS milling centre (Fig. 1). The machine has a maximum rotational speed of 24,000 rpm, which allows for conducting milling processes at a very high cutting speed.

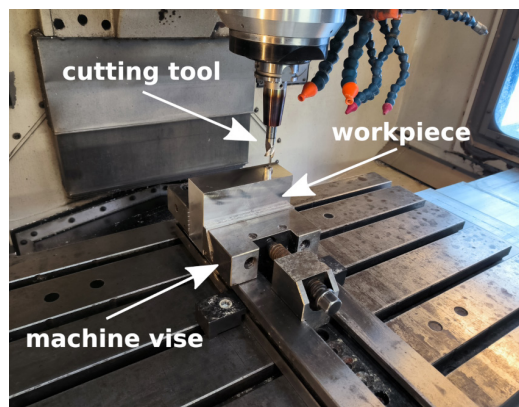


Fig. 1. Experimental setup

Milling tests were performed with the use of two cutting tools with two different types of coating:  $TiB_2$  and  $TiAlN$ . These coatings are dedicated to the machining of magnesium alloys. The tools were AM3SSD1600A100 Mitsubishi end mills, each having a diameter of 16 mm and three cutting edges. The end mills were mounted in Celsio heat-shrinking tool holders from Schunk. To ensure increased stability of the machining process, the holder-tool system was balanced at G2.5 to a speed of 25,000 rpm in compliance with the ISO 21940-1 standard [43].

Apart from the cutting tools, the basic technological parameters of the milling process, i.e., cutting speed  $v_c$ , feed per tooth  $f_z$  and axial depth of cut  $a_p$ , were made variable too. The study was conducted

for 3 levels of variability. In contrast, the radial depth of cut  $a_e$  was constant. A plan of the experiment and values of the milling parameters applied therein are stated in Table 1.

**Table 1.** Plan of the experiment and milling parameters

Cutting tool	$v_c$ [m/min]	$f_z$ [ $\mu\text{m}/\text{tooth}$ ]	$a_p$ [ $\mu\text{m}$ ]	$a_e$ [mm]
TiB <sub>2</sub> -coated,	400	5	80	14
	800			
	1200			
TiAlN-coated	800	1	80	
		5		
	800	9	60	
		5	80	
			100	

Surface quality after the machining tests was examined based on obtained surface roughness profile parameters and Abbott-Firestone curves. Surface roughness was measured using the Hommel Etamic T8000 RC120-400 in compliance with PN-EN ISO 4287 [44] and PN-EN ISO 13565 [45] standards, with a measuring length  $l_n = 4$  mm, a sampling length  $l_r = 0.8$  mm and a traverse speed  $v_t = 0.5$  mm/s. Each measurement was repeated ten times per every machined surface in order to determine mean values and standard deviations. The necessary number of repetitions was previously estimated.

### 3 RESULTS AND DISCUSSION

#### 3.1 Surface Roughness Analysis

The surface quality of the test specimens after precision milling was examined in terms of surface

roughness amplitude parameters  $Ra$ ,  $Rv$ ,  $Rp$ ,  $Rt$  and the functional parameters  $Rvk$ ,  $Rk$ ,  $Rpk$  describing the Abbott-Firestone curve. To illustrate the discussed surfaces, Fig. 2 presents examples of surface topography maps obtained during the milling process with intermediate values of technological parameters and with both cutting tools.

From the isometric images shown, it can be seen that both surfaces have a fairly homogeneous structure, as there are no high peaks or deep valleys, and the tool marks are also small. The surfaces machined with the use of both tools do not differ noticeably from each other. However, a greater share of valleys can be observed on the surface obtained with an end mill with TiAlN coating.

In the following part of the study, an analysis of the effect of changing technological parameters on the surface structure was carried out based on the surface roughness parameters. The influence of cutting speed and type of coating on the mean values of the roughness parameters is presented in Figs. 3 to 5.

The mean values of the  $Ra$  parameter obtained for both end mills were similar, and their range is relatively narrow. During the milling process with the TiB<sub>2</sub>-coated tool, an increase in the cutting speed led to a decrease in the  $Ra$  parameter value first and then to its increase. In contrast, the use of the TiAlN-coated tool led to a decrease in the  $Ra$  parameter over the entire range of tested cutting speed. The results obtained with the TiAlN-coated tool are also characterized by a greater scatter of values.

The results demonstrate that the  $Rv$ ,  $Rp$ , and  $Rt$  parameters depend on cutting speed. In the milling process conducted with the TiB<sub>2</sub>-coated tool, the values of these parameters decreased initially and subsequently increased again with the highest tested cutting speed value. When the milling process was

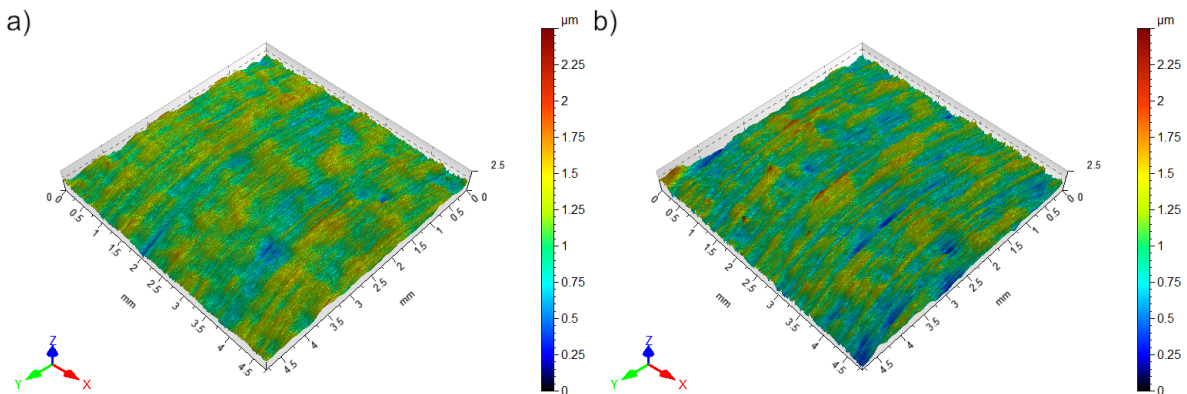


**Fig. 2.** Surface topography maps obtained using; a) TiB<sub>2</sub>-coated, and b) TiAlN-coated tool

performed with the use of the TiAlN-coated tool, these parameters decreased in a roughly linear manner. The peak heights are insignificantly higher than the valley depth, which indicates a relatively symmetric surface roughness profile distribution. As a result of using the TiB<sub>2</sub>-coated tool, the above surface roughness parameters are lower, and the scatter of their values is smaller.

Similar dependencies were also observed for the *Rvk*, *Rk*, and *Rpk* parameters. In the milling process conducted with the TiB<sub>2</sub>-coated tool, an increase in the cutting speed leads to a decrease in these parameters first and then in their increase. When the milling was conducted with the TiAlN-coated tool, values of these parameters decreased throughout the tested cutting speed range. Also, one can again observe a close correlation between the parameters *Rvk* and *Rpk* and the parameters *Rv* and *Rp*. Higher valley depth and peak heights result in higher values of *Rvk* and *Rpk*.

Figs. 6 to 8 show the influence of feed per tooth and tool coating type on the analysed surface roughness parameters.

The effect of feed per tooth on surface roughness is similar, albeit less powerful, to that observed in relation to cutting speed. An analysis of the results also demonstrates that there are greater differences between values of the surface roughness parameters depending on the tool used. The highest values of *Ra* are obtained with the lowest tested feed per tooth value. This suggests that the ploughing phenomenon may occur in this range. For the TiB<sub>2</sub>-coated tool, an increase in the feed per tooth causes a clear decrease in these parameters first and then a slight increase in their values again. The use of the TiAlN-coated tool leads to a steady reduction in their values with increasing the feed per tooth. The decrease in value is associated with a reduction in the ploughing phenomenon and an increasing contribution of the material-cutting process. This phenomenon is typical for precision machining, which is a significant difference from conventional machining.

Similar dependencies can be observed for the *Rv*, *Rp* and *Rt* parameters. Depending on the tool used, their mean values differ more significantly

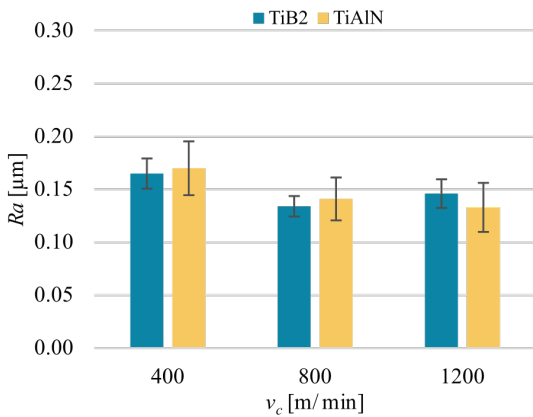


Fig. 3. *Ra* parameter vs. cutting speed  $v_c$

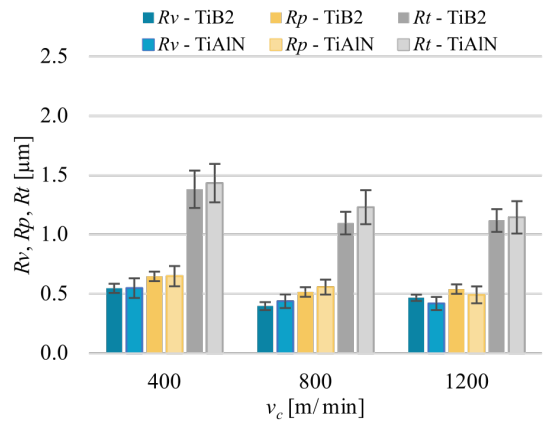


Fig. 4. *Rv*, *Rp* and *Rt* parameters vs. cutting speed  $v_c$

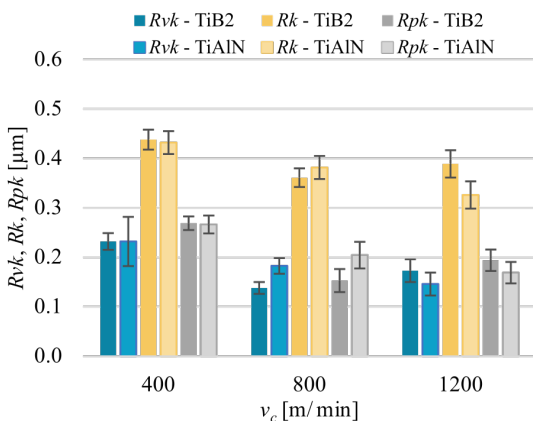


Fig. 5. *Rvk*, *Rk*, and *Rpk* parameters vs. cutting speed  $v_c$

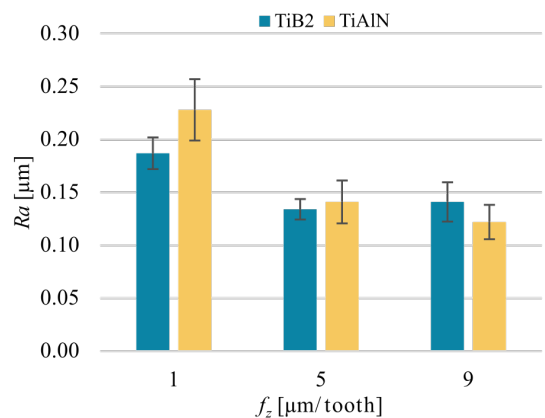


Fig. 6. *Ra* parameter vs. feed per tooth  $f_z$

than those obtained for the variable cutting speed. The highest values are again obtained for the milling process conducted with the lowest tested feed per tooth value. A further increase in the feed per tooth leads to a relatively high decrease in the values of these parameters, followed by their moderate increase. When the TiAlN-coated tool is used, the surface roughness parameters gradually decrease. Although the peak heights are higher, the difference between them and the valley depth is not great, which indicates that the roughness profile distribution was relatively uniform.

The effect of feed per tooth on the  $Rvk$ ,  $Rk$  and  $Rpk$  parameters is similar to that observed for other surface roughness parameters. In the milling process conducted with the TiB<sub>2</sub>-coated tool, the values of these parameters decrease first and then slightly increase. When the milling process is conducted with the TiAlN-coated tool, the surface roughness parameters decrease as the feed per tooth value

increases. Again, one can observe a correlation between  $Rvk$  and  $Rpk$  as well as  $Rv$  and  $Rp$ .

The surface roughness results obtained during machining with a variable axial depth of cut are given in Figs. 9 to 11.

In contrast to the variable cutting speed and feed per tooth, the variable depth of cut has no significant impact on the analysed surface roughness parameters. The mean value of the  $Ra$  parameter remains comparable, irrespective of the applied depth of cut and tool type. Nonetheless, the results obtained for the milling tests carried out with the use of the TiAlN-coated tool are characterized by a greater scatter of values.

A similar trend can be observed for the parameters  $Rv$ ,  $Rp$ , and  $Rt$ . Irrespective of the axial depth of the cut value, the mean values of these parameters are similar. Here again, the peak height is higher than the valley depth. For the milling process conducted with the TiB<sub>2</sub>-coated end mill, the mean values of these

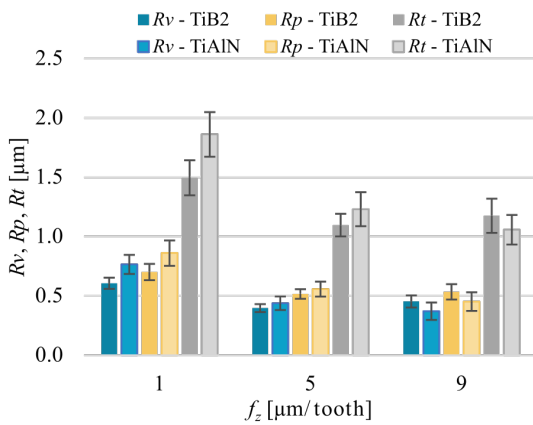


Fig. 7.  $Rv$ ,  $Rp$  and  $Rt$  parameters vs. feed per tooth  $f_z$

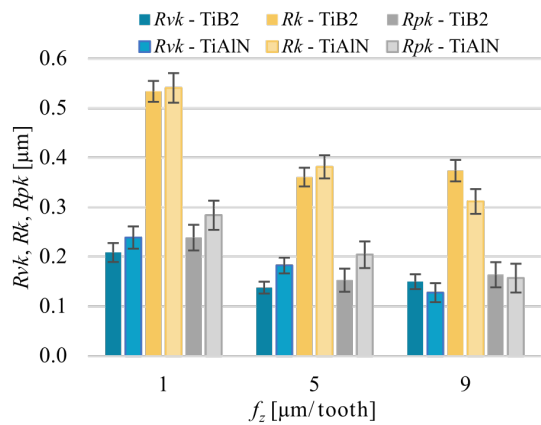


Fig. 8.  $Rvk$ ,  $Rk$ , and  $Rpk$  parameters vs. feed per tooth  $f_z$

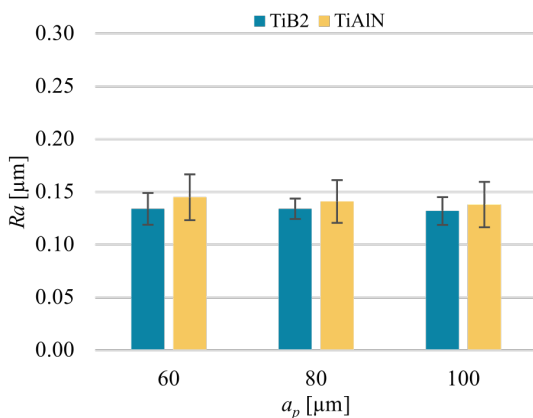


Fig. 9.  $Ra$  parameter vs. axial depth of cut  $a_p$

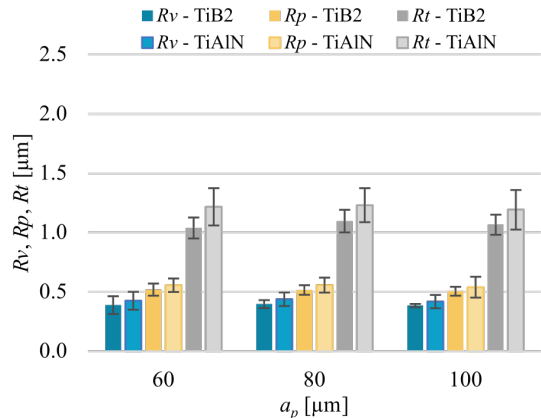
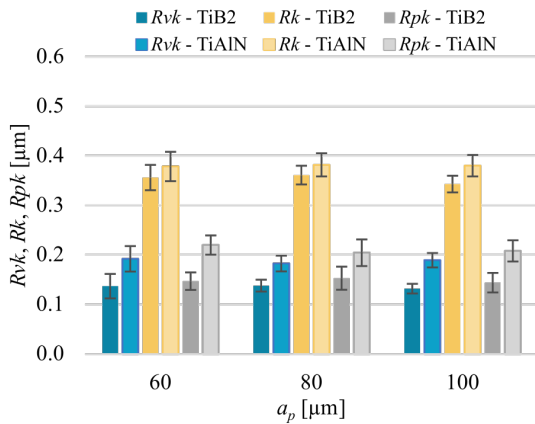


Fig. 10.  $Rv$ ,  $Rp$  and  $Rt$  parameters vs. axial depth of cut  $a_p$

parameters are lower, and the result scatter is smaller, which can best be observed for the  $Rt$  parameter.



**Fig. 11.**  $Rvk$ ,  $Rk$ , and  $Rpk$  parameters vs. axial depth of cut  $a_p$

The variable axial depth of cut has no significant effect on the parameters  $Rvk$ ,  $Rk$ , and  $Rpk$ . The mean values of these parameters are generally similar, and their lower values are received for the surfaces machined with the  $TiB_2$ -coated tool. Here again, one can observe a relationship between  $Rvk$  and  $Rpk$ , as well as  $Rv$  and  $Rp$ . Due to the non-significant effect of the axial depth of the cut, it appears to be possible to increase the process efficiency without a noticeable deterioration in surface quality.

### 3.2 Abbott-Firestone Curves Analysis

During measurements of surface quality, the Abbott-Firestone curves were also obtained. The curves were used to determine the values of the previously analysed parameters  $Rvk$ ,  $Rk$ , and  $Rpk$ . The curves make it possible to determine specifically the functional properties of the surfaces after machining. Examples of the curves obtained for variable milling parameters and both tool coating types are shown in Figs. 12 to 14.

Irrespective of the change in technological parameters and cutting tool, the obtained Abbott-Firestone curves have a similar degressive-progressive pattern. Although all curves have similar inclination angles, the curves obtained from milling with the  $TiAlN$ -coated tool are slightly more inclined. This indicates the presence of sharper peaks, which entails reduced abrasive resistance of the surface. The obtained Abbott-Firestone curves have a roughly symmetric distribution, which is confirmed by the fact that the parameters  $Rvk$  and  $Rpk$  have similar values. The surfaces generated during milling are devoid of high peaks and deep valleys, and the core roughness depth predominates.

An analysis of the Abbott-Firestone curves obtained from milling with the  $TiB_2$ -coated tool also reveals a greater concentration of the material in the core area. This implies that the abrasion period will

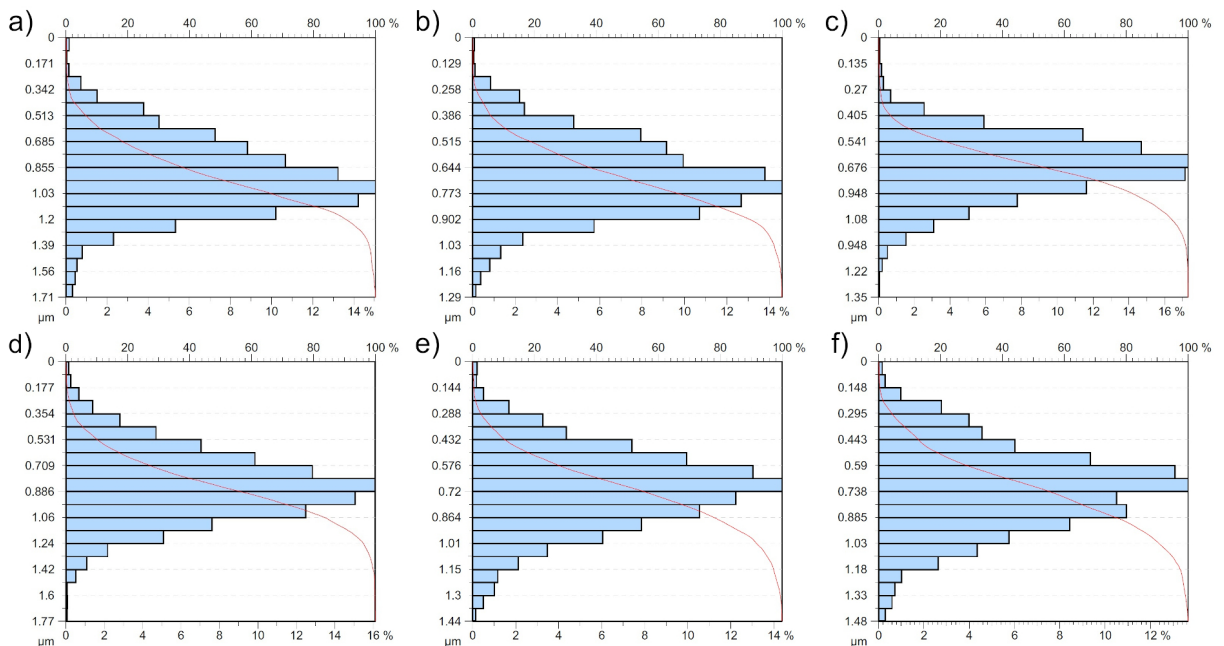


**Fig. 12.** Abbott-Firestone curves obtained from milling with a  $TiB_2$ -coated tool: a)  $v_c = 400$  m/min, b)  $v_c = 800$  m/min, c)  $v_c = 1200$  m/min; and with a  $TiAlN$ -coated tool: d)  $v_c = 400$  m/min, e)  $v_c = 800$  m/min, f)  $v_c = 1200$  m/min

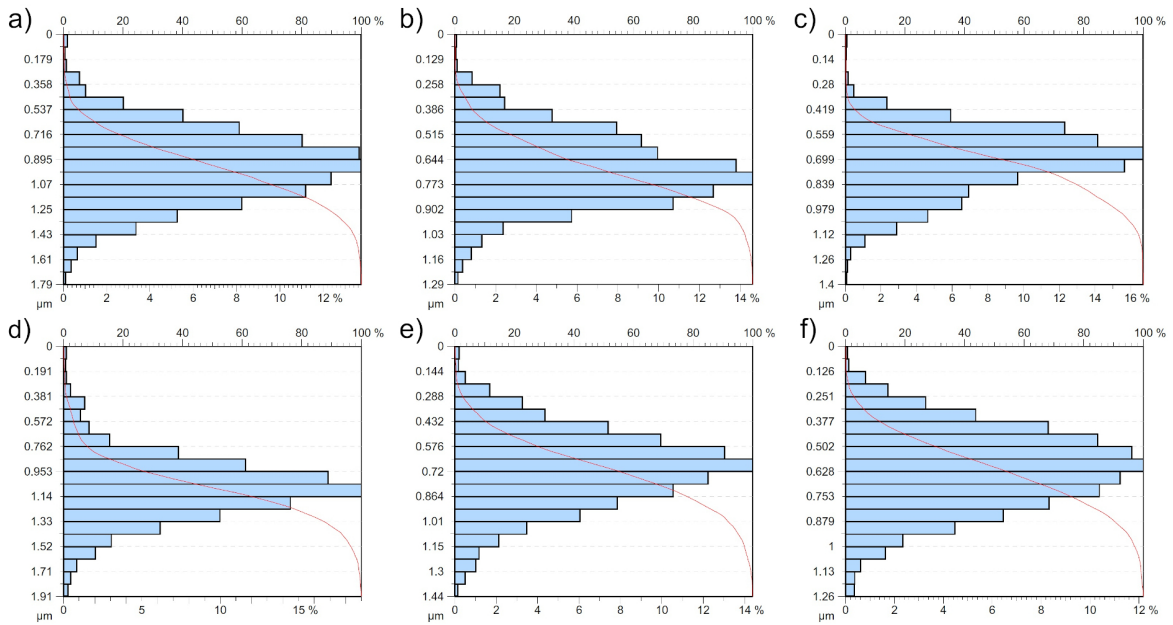


**Fig. 13.** Abbott-Firestone curves obtained from milling with a  $TiB_2$ -coated tool: a)  $f_z = 1 \mu\text{m/tooth}$ , b)  $f_z = 5 \mu\text{m/tooth}$ , c)  $f_z = 9 \mu\text{m/tooth}$ ; and with a  $TiAlN$ -coated tool: d)  $f_z = 1 \mu\text{m/tooth}$ , e)  $f_z = 5 \mu\text{m/tooth}$ , f)  $f_z = 9 \mu\text{m/tooth}$

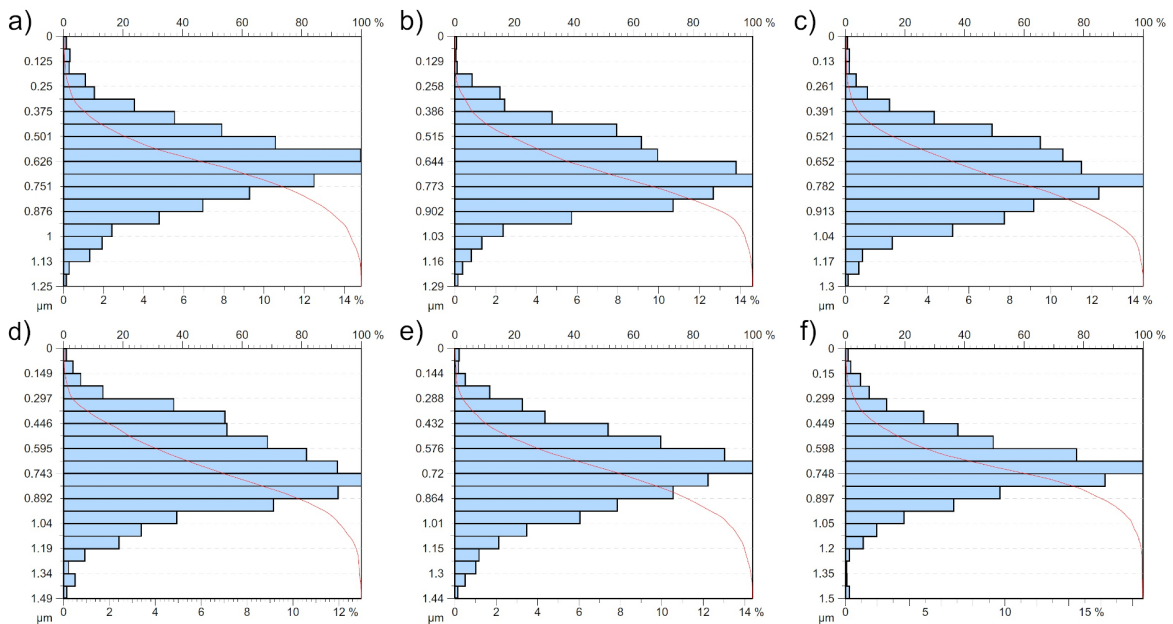


**Fig. 14.** Abbott-Firestone curves obtained from milling with a  $TiB_2$ -coated tool: a)  $a_p = 60 \mu\text{m}$ , b)  $a_p = 80 \mu\text{m}$ , c)  $a_p = 100 \mu\text{m}$ ; and with a  $TiAlN$ -coated tool: d)  $a_p = 60 \mu\text{m}$ , e)  $a_p = 80 \mu\text{m}$ , f)  $a_p = 100 \mu\text{m}$

be shorter due to the lack of high peaks. As for the  $TiAlN$ -coated tool, the material is more spread over the entire roughness profile height. Consequently, the values of  $Rvk$  and  $Rpk$  parameters are higher than those obtained with the  $TiB_2$ -coated tool. High peaks will result in faster abrasion. In contrast, deep valleys encourage the accumulation of lubricant,

which reduces friction and facilitates the movement of cooperating surfaces. In terms of the variable milling parameters, the Abbott-Firestone curves only reveal the presence of small changes in the area size of valley depths, core roughness and peak heights. No significant changes can, however, be observed in the patterns of these curves, which means that the surface



quality and, thus, its functional properties have not undergone any profound changes. Therefore, by modifying the machining conditions, it is feasible to attempt to reduce the values of the preferred surface roughness parameters without compromising the functional properties of the surfaces.

### 3.3 ANOVA Analysis

The obtained results were also analysed statistically using ANOVA with an assumed level of confidence  $\alpha = 0.05$ . The analysis was performed using Statistica 13 software. The analysis determined the significance of the effect of changing individual technological parameters and the tool coating type on surface roughness parameters. The results of the analysis are presented in Tables 2 to 4.

**Table 2.** ANOVA results for variable cutting speed

	Factor	SS	df	MS	F	p
Ra	$v_c$	0.011	2	0.006	15.879	0.000
	Coating	0.000	1	0.000	0.005	0.946
	Total	0.011	3	0.006		
Rv	$v_c$	0.190	2	0.095	31.471	0.000
	Coating	0.000	1	0.000	0.017	0.898
	Total	0.190	3	0.095		
Rp	$v_c$	0.204	2	0.102	27.219	0.000
	Coating	0.000	1	0.000	0.013	0.908
	Total	0.204	3	0.102		
Rt	$v_c$	0.912	2	0.456	25.336	0.000
	Coating	0.075	1	0.075	4.153	0.046
	Total	0.986	3	0.531		
Rvk	$v_c$	0.069	2	0.035	37.914	0.000
	Coating	0.001	1	0.001	0.565	0.456
	Total	0.070	3	0.035		
Rk	$v_c$	0.068	2	0.034	39.460	0.000
	Coating	0.004	1	0.004	4.510	0.038
	Total	0.072	3	0.038		
Rpk	$v_c$	0.102	2	0.051	71.800	0.000
	Coating	0.001	1	0.001	1.324	0.255
	Total	0.103	3	0.052		

Sum-of-squares (SS), Degrees of freedom (df), Mean squares (MS), F ratio (F), and p-value (p).

The performed statistical analysis confirmed that the change in cutting speed had a statistically significant effect on the mean values of all analysed surface roughness parameters ( $p < 0.05$ ). By changing them, it is, therefore, possible to impact the surface roughness. It was also shown that the tool coating type had no statistically significant effect on roughness parameters. The results obtained were, therefore,

similar for both cutting tools. The exceptions were the *Rt* and *Rk* parameters, where the type of coating had a significant effect on their mean values measured on the machined surfaces.

**Table 3.** ANOVA results for variable feed per tooth

	Factor	SS	df	MS	F	p
Ra	$f_z$	0.071	2	0.036	69.907	0.000
	Coating	0.001	1	0.001	2.744	0.103
	Total	0.073	3	0.037		
Rv	$f_z$	0.980	2	0.490	81.671	0.000
	Coating	0.023	1	0.023	3.866	0.054
	Total	1.004	3	0.513		
Rp	$f_z$	0.963	2	0.482	61.847	0.000
	Coating	0.023	1	0.023	2.979	0.090
	Total	0.987	3	0.505		
Rt	$f_z$	3.885	2	1.943	64.165	0.000
	Coating	0.243	1	0.243	8.021	0.006
	Total	4.128	3	2.186		
Rvk	$f_z$	0.078	2	0.039	75.703	0.000
	Coating	0.005	1	0.005	8.839	0.004
	Total	0.083	3	0.044		
Rk	$f_z$	0.428	2	0.214	265.190	0.000
	Coating	0.001	1	0.001	1.280	0.263
	Total	0.429	3	0.215		
Rpk	$f_z$	0.116	2	0.058	66.380	0.000
	Coating	0.013	1	0.013	15.345	0.000
	Total	0.129	3	0.071		

**Table 4.** ANOVA results for variable axial depth of cut

	Factor	SS	df	MS	F	p
Ra	$a_p$	0.000	2	0.000	0.343	0.711
	Coating	0.001	1	0.001	3.237	0.077
	Total	0.001	3	0.001		
Rv	$a_p$	0.003	2	0.001	0.436	0.649
	Coating	0.020	1	0.020	6.674	0.012
	Total	0.023	3	0.022		
Rp	$a_p$	0.003	2	0.001	0.446	0.642
	Coating	0.020	1	0.020	6.170	0.016
	Total	0.023	3	0.022		
Rt	$a_p$	0.017	2	0.008	0.527	0.593
	Coating	0.318	1	0.318	20.191	0.000
	Total	0.334	3	0.326		
Rvk	$a_p$	0.000	2	0.000	0.347	0.708
	Coating	0.041	1	0.041	126.588	0.000
	Total	0.041	3	0.041		
Rk	$a_p$	0.001	2	0.000	0.920	0.404
	Coating	0.011	1	0.011	20.310	0.000
	Total	0.012	3	0.011		
Rpk	$a_p$	0.001	2	0.000	0.599	0.553
	Coating	0.059	1	0.059	125.954	0.000
	Total	0.060	3	0.060		

The analysis also confirmed a significant effect of the change in feed per tooth for all the analysed surface roughness parameters. In this case, the tool coating type was also more important, proving to be significant for the  $R_t$ ,  $R_{vk}$  and  $R_{pk}$  parameters. However, for the other parameters, the tool coating type had no significant effect on the mean values of surface roughness parameters.

A completely opposite relationship occurred for the results obtained when the precision milling process was performed with a variable axial depth of cut. ANOVA results indicated that the change in the depth of cut had no significant effect on any of the analysed surface roughness parameters. However, the type of coating proved to be significant in this case, and it influenced the mean values of measured roughness parameters. The only exception was the  $R_a$  parameter, for which the tool coating type was not significant.

From the performed statistical analysis, it can be concluded that the change in cutting speed and feed per tooth had the greatest influence on the roughness parameters measured on the machined surfaces. However, the change in axial depth was not significant, which makes it possible to increase machining efficiency without any deterioration in surface quality. The significance of the tool coating type depends on the changed cutting parameter.

#### 4 CONCLUSIONS

This experimental study and its findings made it possible to evaluate the surface quality of AZ91D magnesium alloy specimens after precision milling. The results demonstrated that the effect of the applied machining conditions on the analysed surface roughness parameters depended on the tool coating type. The only exception was the variable axial depth of cut because changes in its value did not have any significant effect on the obtained surface quality, irrespective of the tool coating type. Cutting speed and feed per tooth were the most significant factors, which resulted in a reduction in roughness parameters by up to 52 %. Whereas in milling conducted with the TiAlN-coated tool, the use of variable cutting speed and feed always led to a gradual decrease in the surface roughness parameters. In contrast, when the machining was performed with the TiB<sub>2</sub>-coated tool, the surface roughness parameters decreased first and then increased again. For this reason, it appears to be preferable to use intermediate machining conditions for the TiB<sub>2</sub> tool, whereas the highest parameters for the TiAlN tool. Still, the mean values of the surface

roughness parameters in the most optimal conditions were mostly similar for both tool coating types, and their differences did not exceed 16 %. This is also confirmed by the ANOVA analysis. A definite indication of a tool coating type providing better results is, therefore, not possible. Similar surface roughness can be achieved with both coatings. The results obtained for the surface machined with the TiB<sub>2</sub>-coated tool were, however, characterised by a smaller scatter of values. An analysis of the Abbott-Firestone curves demonstrated that the cutting parameters and the type of tool coating had no significant effect on the surface roughness profile shape. Small changes were only observed for the curves describing the parameters  $R_{vk}$ ,  $R_k$ , and  $R_{pk}$ . Nonetheless, those changes were too small to have any profound impact on the functional properties of the surface. The relatively small inclination angle of the Abbott-Firestone curves indicates that the surfaces after precision machining have reasonably high abrasion resistance. The obtained surface structure and low roughness parameters values confirm that the precision milling process can be successfully used to manufacture magnesium alloy components characterised by a high surface quality.

In future studies, the number of analysed values of technological parameters for which machining will be carried out should be increased. This will enable a more accurate determination of the effect of varying machining conditions on surface roughness. The extension of the research will also enable optimisation of the machining conditions in order to achieve the highest possible surface quality. Collecting more information will also enable the process to be optimised by simulating test results.

#### 5 ACKNOWLEDGEMENTS

This research was financed by the Mechanical Engineering Discipline Fund of Lublin University of Technology (Grant No. FD-20/IM-5/060).

#### 6 REFERENCES

- [1] Gobivel, K., Vijay Sekar, K.S. (2022). Influence of cutting parameters on end milling of magnesium alloy AZ31B. *Materials Today: Proceedings*, vol. 62, p. 933-937, DOI:10.1016/j.matpr.2022.04.075.
- [2] Karkalos, N.E., Karmiris-Obratański, P., Kurpiel, S., Zagórski, K., Markopoulos, A.P. (2021). Investigation on the surface quality obtained during trochoidal milling of 6082 aluminum alloy. *Machines*, vol. 9, no. 4, art. ID 75, DOI:10.3390/machines9040075.

- [3] Kuczmaszewski, J., Pieško, P., Zawada-Michałowska, M. (2016.) Surface roughness of thin-walled components made of aluminium alloy EN AW-2024 following different milling strategies. *Advances in Science and Technology Research Journal*, vol. 10, no. 30, p. 150-158, DOI:10.12913/22998624/62515.
- [4] Natarajan, M., Chinnasamy, B., Bejaxhin Alphonse, B. (2022). Investigation of machining parameters in thin-walled plate milling using a fixture with cylindrical support heads. *Strojníški vestnik - Journal of Mechanical Engineering*, vol. 68, no. 12, p. 746-756, DOI:10.5545/sv-jme.2022.273.
- [5] Dung, H., Nguyen, N., Quy, T., Thien, N. (2019). Cutting forces and surface roughness in face-milling of SKD61 hard steel. *Strojníški vestnik - Journal of Mechanical Engineering*, vol. 65, no. 6, p. 375-385, DOI:10.5545/sv-jme.2019.6057.
- [6] Pradeep Kumar, M., Venkatesan, R., Manimurugan, M. (2022). Optimization of process parameters in turning of magnesium AZ91D alloy for better surface finish using genetic algorithm. *Acta Innovations*, vol. 43, p. 54-62, DOI:10.32933/ActaInnovations.43.5.
- [7] Zagórski, I., Szczepaniak, A., Kulisz, M., Korpysa, J. (2022). Influence of the tool cutting edge helix angle on the surface roughness after finishing milling of magnesium alloys. *Materials*, vol. 15, no. 9, art. ID 3184, DOI:10.3390/ma15093184.
- [8] Grzesik, W. (2015). Effect of the machine parts surface topography features on the machine service. *Mechanik*, vol. 8-9, p. 587-593, DOI:10.17814/mechanik.2015.8-9.493. (in Polish)
- [9] Sedlaček, M., Vilhena, L.M.S., Podgornik, B., Vižintin, J. (2011). Surface topography modelling for reduced friction. *Strojníški vestnik - Journal of Mechanical Engineering*, vol. 57, no. 9, p. 674-680, DOI:10.5545/sv-jme.2010.140.
- [10] Grobelny, P., Legutko, S., Habrat, W., Furmański, L. (2018). Investigations of surface topography of titanium alloy manufactured with the use of 3D print. *IOP Conference Series: Materials Science and Engineering*, vol. 393, art. ID 012108, DOI:10.1088/1757-899X/393/1/012108.
- [11] Pawlus, P., Reizer, R., Wieczorowski, M. (2021). Functional importance of surface texture parameters. *Materials*, vol. 14, no. 18, art. ID 5326, DOI:10.3390/ma14185326.
- [12] Skoczylas, A., Zaleski, K., Matuszak, J., Ciecieląg, K., Zaleski, R., Gorgol, M. (2022). Influence of slide burnishing parameters on the surface layer properties of stainless steel and mean positron lifetime. *Materials*, vol. 15, no. 22, art. ID 8131, DOI:10.3390/ma15228131.
- [13] Sathyamoorthy, V., Deepan, S., Sathya Prasanth, S.P., Prabhu, L. (2017). Optimization of machining parameters for surface roughness in end milling of magnesium AM60 alloy. *Indian Journal of Science and Technology*, vol. 10, no. 32, p. 1-7, DOI:10.17485/ijst/2017/v10i32/104651.
- [14] Alharti, N.H., Bingol, S., Abbas, A.T., Ragab, A.E., El-Danaf, E.A., Alharbi, H.F. (2017). Optimizing cutting conditions and prediction of surface roughness in face milling of AZ61 using regression analysis and artificial neural network. *Advances in Materials Science and Engineering*, vol. 2017, art. ID 7560468, DOI:10.1155/2017/7560468.
- [15] Chirita, B., Grigoras, C., Tampu, C., Herghelegiu, E. (2019). Analysis of cutting forces and surface quality during face milling of a magnesium alloy. *IOP Conference Series: Materials Science and Engineering*, vol. 591, art. ID 012006, DOI:10.1088/1757-899X/591/1/012006.
- [16] Ruslan, M.S., Othman, K., Ghani, J.A., Kassim, M.S., Haron, C.H. (2016). Surface roughness of magnesium alloy AZ91D in high speed milling. *Jurnal Teknologi*, vol., 78, no. 6-9, p. 115-119, DOI:10.11113/jt.v78.9158.
- [17] Kim, J.D., Lee, K.B. (2010). Surface roughness evaluation in dry-cutting of magnesium alloy by air pressure coolant. *Engineering*, vol. 2, no. 10, p. 788-792, DOI:10.4236/eng.2010.210101.
- [18] Shi, K., Zhang, D., Ren, J., Yao, C., Huang, X. (2016). Effect of cutting parameters on machinability characteristics in milling of magnesium alloy with carbide tool. *Advances in Mechanical Engineering*, vol. 8, no. 1, p. 1-9, DOI:10.1177/1687814016628392.
- [19] Chhetir, S., Tariq, M., Mohapatra, S., Sumi, V., Zhimomi, A., Davis, R., Singh, A. (2020). Surface characteristics enhancement of biocompatible Mg alloy AZ31B by cryogenic milling. *IOP Conference Series: Materials Science and Engineering*, vol. 1004, art. ID 012011, DOI:10.1088/1757-899X/1004/1/012011.
- [20] Sivam, S.P., Bhat, M.D., Natarajan, S., Chauhan, N. (2018). Analysis of residual stresses, thermal stresses, cutting forces and other output responses of face milling operation on ZE41 magnesium alloy. *International Journal of Modern Manufacturing Technologies*, vol. 10, no. 1, p. 92-101.
- [21] Kumar, R., Katyal, P., Kumar, K. (2023). Effect of end milling process parameters and corrosion behaviour of ZE41A magnesium alloy using Taguchi based GRA. *Biointerface Research in Applied Chemistry*, vol. 13, no. 3, art. ID 214, DOI:10.33263/briac133.214.
- [22] Muralidharan, S., Karthikeyan, N., Kumar, A.B., Aatthisugan, I.A. (2017). A study on machinability characteristic in end milling of magnesium composite. *International Journal of Mechanical Engineering and Technology*, vol. 8, no. 6, p. 455-462.
- [23] Marakini, V., Pai, S., Bhat, U., Singh, D., Achar, B. (2022). High speed machining for enhancing the AZ91 magnesium alloy surface characteristics: Influence and optimisation of machining parameters. *Defence Science Journal*, vol. 72, no. 1, p. 105-113, DOI:10.14429/dsj.72.17049.
- [24] Marakini, V., Pai, S., Bhat, A., Bangera, S. (2022). Surface integrity optimization in high speed milling of AZ91 magnesium alloy using TOPSIS considering vibration signals. *Materials Today: Proceedings*, vol. 52, p. 802-809, DOI:10.1016/j.matpr.2021.10.154.
- [25] Zagórski, I., Korpysa, J. (2019). Surface quality in milling of AZ91D magnesium alloy. *Advances in Science and Technology Research Journal*, vol. 13, no. 2, p. 119-129, DOI:10.12913/22998624/108547.
- [26] Guo, Y.B., Salahshoor, M. (2010). Process mechanics and surface integrity by high-speed dry milling of biodegradable magnesium-calcium implant alloys. *CIRP Annals*, vol. 59, no. 1, p. 151-154, DOI:10.1016/j.cirp.2010.03.051.

- [27] Salahshoor, M., Guo, Y.B. (2011). Surface integrity of magnesium-calcium implants processed by synergistic dry cutting-finish burnishing. *Procedia Engineering*, vol. 19, p. 288-293, DOI:10.1016/j.proeng.2011.11.114.
- [28] Salahshoor, M., Guo, Y.B. (2011). Cutting mechanics in high speed dry machining of biomedical magnesium-calcium alloy using internal state variable plasticity model. *International Journal of Machine Tools and Manufacture*, vol. 51, no. 7-8, p. 579-590, DOI:10.1016/j.ijmactools.2011.04.004.
- [29] Qiao, Y., Wang, S., Guo, P., Yang, X., Wang, Y. (2018). Experimental research on surface roughness of milling medical magnesium alloy. *IOP Conference Series: Materials Science and Engineering*, vol., 397, art. ID 012114, DOI:10.1088/1757-899X/397/1/012114.
- [30] Desai, S., Malvade, N., Pawade, R., Warhatkar, H. (2017). Effect of high speed dry machining on surface integrity and biodegradability of Mg-Ca1.0 biodegradable alloy. *Materials Today: Proceedings*, vol. 4, no. 6, p. 6817-6727, DOI:10.1016/j.matpr.2017.06.447.
- [31] Jouini, N., Ruslan, M.S.M., Ghani, J.A., Haron, C.H.C. (2023). Sustainable high-speed milling of magnesium alloy AZ91D in dry and cryogenic conditions. *Sustainability*, vol. 15, no. 4, art. ID 3760, DOI:10.3390/su15043760.
- [32] Kanan, M., Zahoor, S., Habib, M.S., Ehsan, S., Rehman, M., Shahzaib, M., Khan, S.A., Ali, H., Abusaq, Z., Hamdan, A. (2023). Analysis of carbon footprints and surface quality in green cutting environments for the milling of AZ31 magnesium alloy. *Sustainability*, vol. 15, no. 7, art. ID 6301, DOI:10.3390/su15076301.
- [33] Buk, J. (2022). Surface Topography of Inconel 718 alloy in finishing WEDM. *Advances in Science and Technology Research Journal*, vol. 16, no. 1, p. 47-61, DOI:10.12913/22998624/142962.
- [34] Skoczylas, A., Zaleski, K. (2019). Effect of centrifugal shot peening on the surface properties of laser-cut C45 steel parts. *Materials*, vol. 12, no. 21, art. ID 3635, DOI:10.3390/ma12213635.
- [35] Pisula, J., Budzik, G., Przeszlowski, Ł. (2019). An analysis of the surface geometric structure and geometric accuracy of cylindrical gear teeth manufactured with the direct metal laser sintering (DMLS) method. *Strojnicki vestnik - Journal of Mechanical Engineering*, vol. 65, no. 2, p. 78-86, DOI:10.5545/sv-jme.2018.5614.
- [36] Zagórski I., Korpysa, J. (2020). Surface quality assessment after milling AZ91D magnesium alloy using PCD tool. *Materials*, vol. 13, no. 3, art. ID 617, DOI:10.3390/ma13030617.
- [37] Kulisz, M., Zagórski, I., Matuszak, J., Klonica, M. (2019). Properties of the surface layer after trochoidal milling and brushing: experimental study and artificial neural network simulation. *Applied Sciences*, vol. 10, no. 1, art. ID 75, DOI:10.3390/app10010075.
- [38] Karmiris-Obratański, P., Karkalos, N.E., Kudelski, R., Markopoulos, A.P. (2022). Experimental study on the effect of the cooling method on surface topography and workpiece integrity during trochoidal end milling of Incoloy 800. *Tribology International*, vol. 176, art. ID 107899, DOI:10.1016/j.triboint.2022.107899.
- [39] Zaleski, K., Matuszak, J., Zaleski, R. (2018). *Surface Layer Metrology*, Lublin University of Technology Publishing House, Lublin.
- [40] Wieczorowski, M. (2009). *Use of Topographic Analysis in the Measurement of Surface Irregularities*. Publishing House of Poznan University of Technology, Poznan.
- [41] Sedlaček, M., Gregorčič, P., Podgornik, B. (2017). Use of the roughness parameters Ssk and Sku to control friction - a method for designing surface texturing. *Tribology Transactions*, vol. 60, no. 2, p. 260-266, DOI:10.1080/10402004.2016.1159358.
- [42] El-Shenawy, E.H., Farahat, A.I.Z. (2023). Surface quality and dry sliding wear behavior of AZ61Mg alloy using Abbott firestone technique. *Scientific Reports*, vol. 13, art. ID 12437, DOI:10.1038/s41598-023-39413-x.
- [43] ISO 21940-1:2019. *Mechanical vibration - Rotor balancing - Part 1: Introduction*, International Organization for Standardization, Geneva.
- [44] ISO 4287:1999. *Geometrical Product Specifications (GPS) - Surface texture: Profile method - Terms, definitions and surface texture parameters*. International Organization for Standardization, Geneva.
- [45] ISO 13565-2:1996. *Geometrical Product Specifications (GPS) - Surface texture: Profile method; Surfaces having stratified functional properties*. International Organization for Standardization, Geneva.